



## Review

## Point defect properties in hcp and bcc Zr with trace solute Nb revealed by ab initio calculations

X.K. Xin, W.S. Lai\*, B.X. Liu

Laboratory of Advanced Materials, Department of Materials Science and Engineering, Tsinghua University, Beijing 100084, China

## ARTICLE INFO

## Article history:

Received 19 January 2009

Accepted 3 June 2009

## ABSTRACT

The properties of simple point defect (i.e. vacancy, self and foreign interstitial atoms) in the hcp (alpha) and bcc (beta) Zr with trace solute Nb have been studied by ab initio calculations with VASP codes. The calculations indicate that the formation energies of vacancy and substitutional Nb atom are 1.94 eV and 0.68 eV in alpha Zr and 0.36 eV and 0.07 eV in beta Zr, respectively, while the binding energies of the nearest neighbor vacancy–substitutional Nb pair and the nearest neighbor substitutional Nb–Nb pair are 0.09 eV and 0.03 eV in alpha Zr and 2.78 eV and 0.72 eV in beta Zr, respectively. These results suggest that the Nb atoms are more likely to agglomerate and form precipitates in the beta Zr than in the alpha Zr. Thus, the  $\alpha$ -Zr- $\beta$ -Zr- $\beta$ -Nb transition mechanism through in situ  $\alpha$  to  $\beta$  transformation of Zr and the vacancy-assisted Nb diffusion for Nb conglomeration in beta Zr under irradiation is proposed to explain the existence of beta Nb and Zr precipitate mixtures observed in the experiments for the Zr–Nb alloy. In addition, the defect formation energies in bcc Nb are also presented.

© 2009 Elsevier B.V. All rights reserved.

## Contents

1. Introduction .....	197
2. Calculation method .....	198
3. Results and discussion .....	199
4. Conclusions .....	201
Acknowledgement .....	202
References .....	202

## 1. Introduction

Zirconium based alloys with niobium are widely used as cladding materials in nuclear reactors recently, e.g. M5<sup>TM</sup> (a Zr–1 wt% Nb–O alloy, very similar to the Russian's E110 alloy) [1], ZIRLO<sup>TM</sup> (a Zr–Nb–Sn–Fe alloy) [2] and Zr–2.5 wt%Nb–O alloys which has been used for pressure tube materials in the CANDU<sup>TM</sup> reactors in Canada [3]. The understanding of corrosion behavior and mechanisms of these alloys under irradiation circumstance is very important for the lifetime prolongation and safety of the materials. It is believed that trace niobium plays an important role in improving the corrosion resistance of the alloy [4,5]. A lot of researches have been done mainly on Zr–2.5Nb alloy to investigate the relationship of Nb and corrosion resistance. For instance, Urbanic

et al. suggested that one of the most important factors leading to improved corrosion properties in Zr–2.5Nb might be the precipitation of beta Nb particles and the consequent reduction of Nb in the alpha Zr grains during irradiations [6]. Jeong suggested that the equilibrium concentration of Nb in the alpha Zr would be a more dominant factor to enhance the corrosion resistance than the precipitates containing Nb, supersaturated Nb, and beta phase [7]. Although the detailed mechanism of this improvement is still not well investigated, it is convinced that the precipitation of beta Nb is related to the corrosion resistance of the Zr based alloy.

It was assumed that the precipitation of niobium could be achieved by two mechanisms. One was that niobium atoms substituted the position of the alpha Zr atoms to form an alpha Nb nucleus, and then change to a beta Nb structure after its growth to some critical size. Another mechanism was that some grains of alpha Zr transformed into beta Zr under irradiation and niobium atoms took the position of the beta Zr atoms to form a beta Nb structure. Experimental results have proved the existence of

\* Corresponding author. Tel.: +86 10 62782370; fax: +86 10 62771160.  
E-mail address: [wslai@tsinghua.edu.cn](mailto:wslai@tsinghua.edu.cn) (W.S. Lai).

needle like beta phase Zr with about 20–88% Nb under irradiation conditions [8–12], lending a support for the possibility of the second mechanism. Nevertheless, no direct experimental evidence has been found to support or deny the first mechanism. The computer simulations which have already been used to investigate the behavior and mechanism of Nb and Fe in Zr alloy [13,14] will be helpful to clarify the possibility of the two precipitation mechanisms. It is known that the formation of Nb precipitates is correlated to the creation and movement of point defects under irradiation circumstance. Therefore, to clarify the above issue, it is important to know the formation and binding energies of the point defects in hcp and bcc Zr with trace solute Nb, which are still lacking.

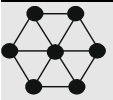
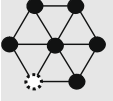
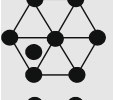
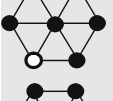



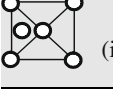

The formation energies of point defects in pure Zr have been calculated in previous researches [15,16]. In the present study, we employ the Vienna Ab initio Simulation Package (VASP) [17,18] to investigate the interactions between Nb and Nb/Zr atoms in the Zr matrix with either hcp or bcc structure, and to calculate the formation and binding energies of simple defects such as vacancies, interstitial and substitutional atoms in the Zr–Nb alloy. In addition, the formation energy of point defects in bcc niobium phase is also presented. These formation and binding energies of simple defects will help us to understand the niobium precipitate mechanisms and further to investigate the corrosion behavior of the Zr–Nb alloy under irradiation conditions.

## 2. Calculation method

In this work, we employed the VASP code [17,18] to perform calculation. The projector augmented wave (PAW) pseudo potentials were chosen, and the exchanges and correlations were described with the Generalized Gradient Approximation (GGA) for the Zr and Nb atoms. We used two different sized super cells for hcp structure and one super cell for bcc structure. For computational convenience, we employed a cuboid or cubic computational supercell with period boundary conditions, and chose a unit cell with dimensions of  $a$ ,  $\sqrt{3}a$ ,  $c$  ( $a$  and  $c$  are lattice constants) containing 4 atoms in the position of (0 0 0), (0.5 0.5 0), (0 1/3 0.5), and (0.5 5/6 0.5) for hcp structure, and a cubic unit cell with 2 atoms in (0 0 0) and (0.5 0.5 0.5) for bcc structure. The hcp super cells contained 48 atoms and 96 atoms with  $3 \times 2 \times 2$  and  $4 \times 2 \times 3$  unit cells, respectively, and the bcc super cell contained 54 atoms with  $3 \times 3 \times 3$  unit cells. For summation over Brillouin zone, a uniform grid of k-points was chosen according to the Monkhorst-Pack scheme [19] and the number of k-points was sampled by  $3 \times 3 \times 3$  for 48 and 54 atoms super cells and by  $2 \times 2 \times 2$  for 96 atoms, respectively. The plane-wave kinetic energy cutoff was set to 350 eV.

In real situation, a point defect can hardly change the shape of a bulk crystal, so we employed a relaxing scheme without changing the shape of the super cell. The calculations were conducted in

**Table 1**  
The calculated energy values in eV for (i) perfect crystal, (ii) vacancy, (iii) octahedral self interstitial atom (SIA), (iv) substitutional Nb, and (v) octahedral foreign interstitial Nb atom in hcp Zr matrix, and for (vi) perfect crystal, (vii) vacancy, (viii) octahedral SIA, and (ix) tetrahedral SIA in bcc Nb. The data in the first line are obtained in the super cell of 48 atoms for Zr and of 54 atoms for Nb, and those in the second line are for Zr with 96 atoms. Black, white and dotted line circles represent Zr atom, Nb atom and vacancy, respectively.

Configuration	Energy per cell	Energy per atom	Formation energy	Previous works
 (i)	–404.77 –809.47	–8.43 –8.43	–	–8.44 [20]
 (ii)	–394.39 –799.18	–	1.94 1.86	1.86 [15]
 (iii)	–410.30	–	2.89	2.84 [15]
 (iv)	–405.84 –810.56	–	0.68 0.67	0.61 [14]
 (v)	–412.39	–	2.56	2.76 [14]
 (vi)	–550.25	–10.19	–	–10.05 [20]
 (vii)	–537.30	–	2.77	2.75 [21]
 (viii)	–554.87	–	5.57	–
 (ix)	–555.79	–	4.65	–

three steps. First, the positions of the atoms in the super cell were allowed to relax to a state with lowest energy. Then the size of the super cell was rescaled to reach a state with lowest energy. Finally, the above energy relaxation process iterated until the forces on all the atoms were less than  $10^{-3}$  eV/Å and the energy of the relaxed super cell was obtained. The calculated lattice constants are 3.233 and 5.167 Å for perfect hcp Zr, 3.575 Å for perfect bcc Zr and 3.305 Å for perfect bcc Nb after relaxation, which are in good agreement with corresponding experimental and other ab initio calculation values of 3.232, 5.149, 3.574 [20], and 3.301 Å, respectively.

The formation energy was defined to be the energy difference between the energy of the super cell calculated by ab initio method and energy sum of each atom in the reference state, which was the perfect hcp (or bcc) Zr crystal for Zr atoms and the perfect bcc Nb for Nb atoms, respectively. For example, the formation energy of a substitutional Nb atom in a super cell of 48 Zr atoms in hcp structure was the difference between the energy of the super cell and the energy sum of one Nb atom in the bcc state and 47 Zr atoms in perfect hcp crystal.

We employed Domain method [14] to calculate the binding energy of point defects, which is defined to be energy difference between the formation energy of a state containing two interacted defects and sum of that of two states containing respective single defect.

### 3. Results and discussion

Table 1 shows the calculated values for the energies of perfect hcp Zr and bcc Nb crystals and the formation energies of vacancies, a Nb substitutional or interstitial atom in hcp Zr, and comparison with other first-principle calculations. It is seen from Table 1 that in general the value of the formation energies calculated for 48 atoms are larger than that for 96 atoms owing to more sufficient relaxation in the latter case. It is also seen that the present results are compatible with previous calculations. It is noticed from Table 1 that the most stable position for a self interstitial atom (SIA) in bcc Nb is the tetrahedral site, which is somehow different from that observed in hcp Zr where the most stable SIA was in the octahedral position [15]. This arises from the different interstitial spaces between hcp and bcc structures. In hcp structure, the radii of the empty sphere in octahedral and tetrahedral interstitial are  $0.414 r_0$  and  $0.225 r_0$ , respectively, while they are  $0.155 r_0$  and  $0.291 r_0$  in bcc structure, respectively, where  $r_0$  is the radius of the atom in the respective hcp or bcc structure. Thus, the larger the interstitial space is, the more stable SIA becomes. It is also seen from Table 1 that the formation energy of SIA in bcc Nb is larger than that in hcp Zr. This is due to the intrinsic difference between Nb and Zr, plus smaller interstitial space in bcc than in hcp structure.

For a combination of two point defects in hcp Zr, we considered the following configurations:


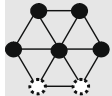
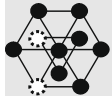
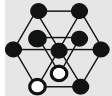
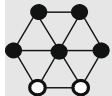
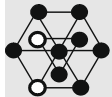


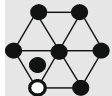

- (a) two nearest neighbor vacancies in the different basal plane,
- (b) two nearest neighbor vacancies in the same basal plane,
- (c) two second nearest neighbor vacancies,
- (d) two nearest neighbor substitutional Nb atoms in the different basal plane,
- (e) two nearest neighbor substitutional Nb atoms in the same basal plane,
- (f) two second nearest neighbor substitutional Nb atoms,
- (g) a substitutional Nb atom–vacancy pair at the nearest neighbor distance in the same basal plane,
- (h) a substitutional Nb atom–vacancy pair at the second nearest neighbor site,

- (i) an octahedral Zr interstitial–substitutional Nb atom pair at the nearest neighbor distance,
- (j) An octahedral Nb interstitial–vacancy pair at the nearest neighbor distance.

The formation and binding energies of various combinations of two point defects mentioned above were calculated in the hcp Zr based super cell of 48 atoms. The results are given in Table 2. The ratio of  $c/a$  calculated (1.598) is less than the theoretical value of 1.633 in Zr, which indicates that the distance of the nearest atoms in the same basal plane is a little larger than that in the different basal plane. Case (a) and (d) are calculated for those atoms in different planes. It can be seen that the formation energy for a defect pair in the case of (b), (c), (d), (e) and (f) are about twice as that of the corresponding simple defect, showing the small binding energy owing to the small relaxations for substitutional atoms and

**Table 2**

The energy values in eV calculated in the hcp Zr super cell of 48 atoms for the first nearest neighbor (NN) vacancies in the different (a) or same, (b) basal plane, the second NN vacancies, (c) the first NN substitutional Nb atoms in the different, (d) or same, (e) basal plane, the second NN substitutional Nb atoms, (f) the first, (g) and second, (h) NN substitutional Nb–vacancy pair, the first NN octahedral Zr interstitial–substitutional Nb pair, (i) and the first NN octahedral Nb interstitial–vacancy pair, (j) Black, white and dotted line circles represent Zr atom, Nb atom and vacancy, respectively.

Configuration	Energy per cell	Formation energy	Binding energy
 (a)	−384.20	3.69	0.18
 (b)	−384.07	3.82	0.05
 (c)	−384.06	3.84	0.04
 (d)	−406.96	1.32	0.04
 (e)	−406.94	1.33	0.03
 (f)	−406.96	1.32	0.04
 (g)	−395.56	2.53	0.09
 (h)	−395.57	2.52	0.10
 (i)	−411.80	3.16	0.42
 (j)	−405.84	0.68	3.82

vacancies. But the formation energy of case (a) is about 0.13 eV lower than that of the case (b) and (c). The formation energy for (g) and (h) are approximately equal to the formation energy of vacancy plus that of substitutional Nb atom, suggesting that there is little binding between substitutional Nb atom and vacancy. The binding energies between vacancies and substitutional atoms are about 0.03–0.10 eV in our calculation. Interestingly, from Table 2 we can see that the formation energy of 3.16 eV for the case of (i) is higher than that of 2.56 eV for octahedral Nb interstitial, suggesting that the energy of system will decrease by 0.60 eV if the positions of Zr and Nb atoms exchange with each other in the octahedral interstitial Zr atom–substitutional Nb atom pair. Moreover, their binding energy is 0.42 eV, indicating that this defect pair is more stable than separate substitutional Nb atom and interstitial Zr atom. Due to this large binding energy, there would be a chance for interstitial Zr and substitutional Nb to stick together, and due to the difference in formation energy between case (i) and interstitial Nb, there would be a chance for Zr interstitial to squeeze out the substitutional Nb atom to form the octahedral Nb interstitial. The radius of an atom played an important role here. It was reported that in the Zr–Fe alloy, the large size Zr interstitial atom would possess the position of small size substitutional Fe atom and squeeze out Fe to interstitial position when they met each other [13]. This will decrease the energy of the system approximately by the amount of interstitial Zr formation energy, since the formation energy of Fe interstitial is almost the same as that of the substitutional Fe atom [13]. Similarly, in the present case (i), the small size Nb atom would also be easier to stay in interstitial position than the large size Zr atom so as to decrease the energy of the system. For the case of (j), the energy of the super cell of 48 atoms was  $-405.84$  eV, which is the same as that for the substitutional Nb atom. To see what has happened for this configuration of (j) by relaxation, the projected diagrams on the  $x$ – $y$  plane before and after relaxation for the super cell containing an interstitial Nb atom close to vacancy are shown in Fig. 1. Both the energy and the figure indicate that the interstitial Nb atom will relax to the vacancy position when it is close to the vacancy rather than possess asymmetrical position near the vacancy as in the case of Fe

[13]. This results in annihilation of the Frenkel pair with alien atom to form the substitutional Nb atom, accompanying with the decrease of the system energy of 3.82 eV as shown as the binding energy in Table 2.

It would be interesting to know the formation and binding energies of simple defects in a beta phase Zr, as the formation of beta phase Zr with about 20–88% Nb under irradiation conditions was observed in the experiments [8–12]. The calculated values in beta phase Zr are given in Table 3. It can be seen that the calculated cohesive energy of beta Zr is compatible with the results reported before [20]. The formation energy of substitutional Nb atom in beta Zr is 0.07 eV, much lower than that of 0.68 eV in alpha Zr, while the binding energy of two nearest neighbor substitutional Nb atoms in beta Zr is 0.72 eV, much higher than that of 0.03 eV in alpha Zr. These results suggested that Nb atoms tend to migrate to the beta phase Zr from alpha phase Zr if some beta Zr grains are formed in the Zr–Nb alloy under irradiation, and that Nb atoms are more likely to agglomerate in beta Zr than in alpha Zr, supposing the Nb atoms could get enough ‘activate energy’ under irradiation. This is consistent with the experiment analysis [12] that the thermal diffusion effect facilitates the supersaturated Nb atoms in the  $\alpha$ -Zr grains to move to the  $\beta$ -Zr, transforming it to the  $\beta$ -Nb. It is also seen from Table 3 that the formation energy of vacancy in beta Zr is 0.36 eV, while it is 1.94 eV in alpha Zr. The calculated binding energy between vacancy and substitutional Nb atom in the first NN, second NN and third NN positions after relaxation are 2.78 eV, 1.03 eV and 0.58 eV respectively, while it is 0.09 eV and 0.10 eV in the first NN and second NN positions in alpha Zr. These results clearly show that the binding energy increases fast when the vacancy approaches the Nb atom in beta Zr. It should be pointed out that significant increase of the binding energy for the first NN substitutional Nb–vacancy pair is partially ascribed to lattice distortion around the pair, as shown in Fig. 2, which reflects the instability of beta Zr at 0 K, as compared with alpha Zr. The low formation energy of vacancy and high binding energy between vacancy and substitutional Nb atom suggest that vacancies are readily formed and easily trapped by Nb atoms in beta Zr. It was reported that in  $\alpha$ -Fe Cu precipitate could trap vacancies owing to small vacancy formation energy in Cu precipitate and with help

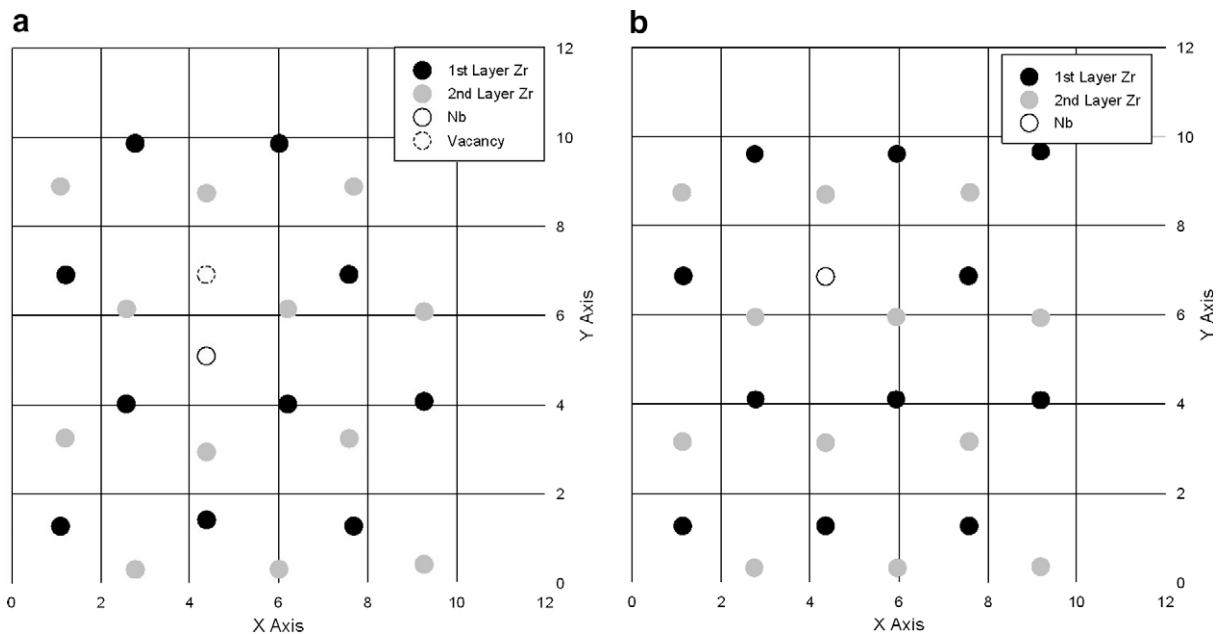
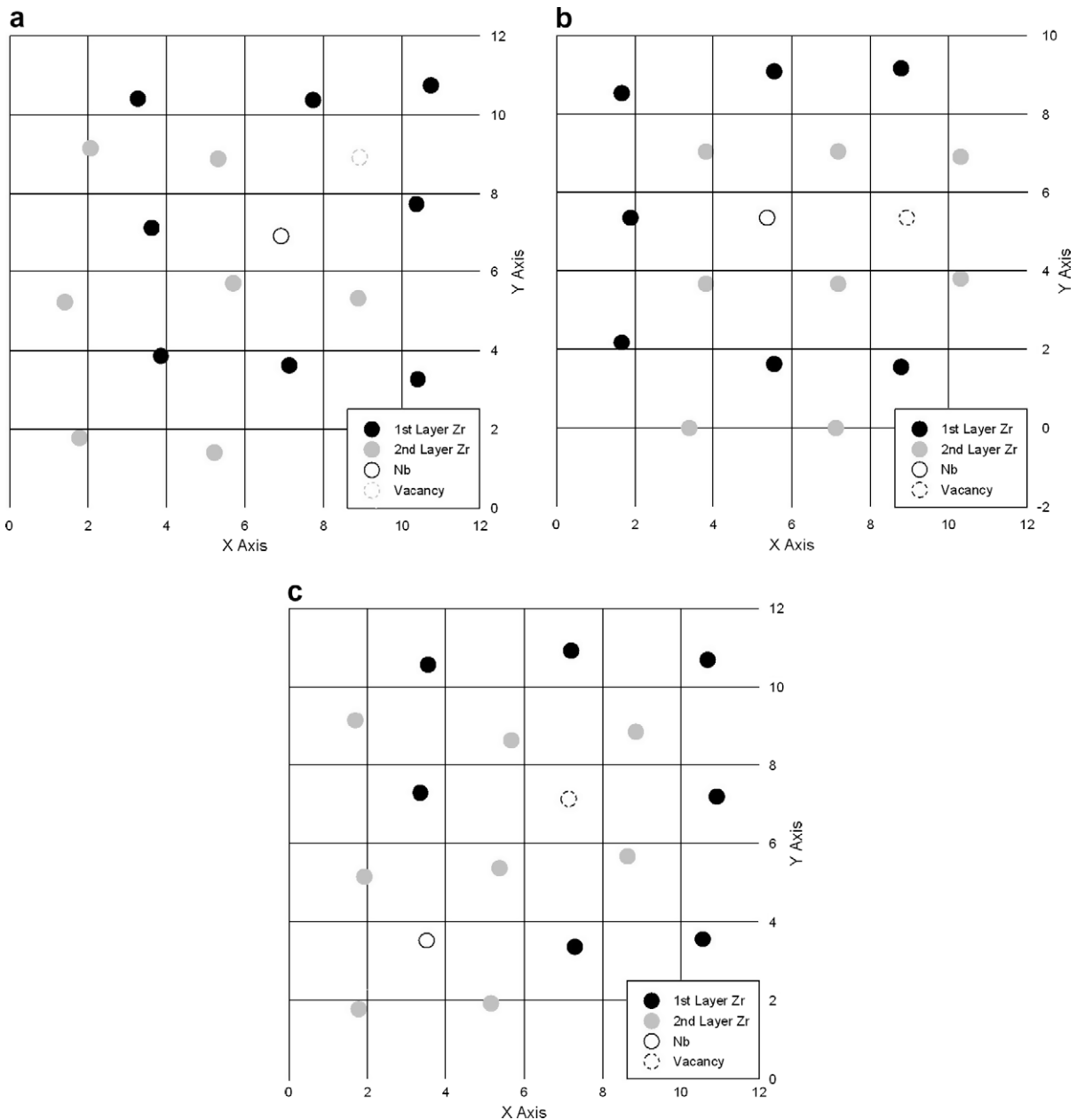


Fig. 1. A projected diagram of super cell on the  $x$ – $y$  plane for Nb interstitial close to the nearest neighbor vacancy in hcp Zr before (a) and after (b) relaxation.










**Fig. 2.** A projected diagram of super cell on the  $x$ - $y$  plane for substitutional Nb atom and vacancy pairs in (a) the first nearest neighbor (NN), (b) the second NN and (c) the third NN positions in bcc Zr after relaxation.

of vacancies Cu cluster up to several tens of Cu atoms can be much more mobile than individual copper atoms [22]. Similarly, in the present case, this vacancy mediated cluster diffusion could happen in beta Zr owing to the strong binding between Nb atoms and vacancies. Thus, the Nb atoms are more easily agglomerating and forming precipitations in the beta Zr than in the alpha Zr through in situ  $\alpha$  to  $\beta$  transformation of Zr and the vacancy-assisted diffusion mechanisms under irradiation. It is still an open question for the detailed Nb diffusion mechanisms in  $\alpha$ -Zr and  $\beta$ -Zr, which needs further study. The appearance of beta Zr under irradiations in the Zr-Nb alloy as mentioned in the experiments [8–12] would highly promote the precipitation of Nb, suggesting that the  $\alpha$ -Zr- $\beta$ -Zr- $\beta$ -Nb transition is a possible way to form Nb precipitates. The observation of mixtures of beta Nb and Zr precipitates together in experiments [8–12] lends a support to the above explanation.

#### 4. Conclusions

The point defect properties in the hcp and bcc Zr with trace Nb were studied using ab initio calculations. The calculated formation energies of simple defects (i.e. vacancy, substitutional atoms, self and foreign interstitial atoms) were found to be in agreement with previous calculations. Defect combinations were investigated to further clarify the behavior of trace Nb in both hcp and bcc structure Zr. The calculations suggested that the  $\alpha$ -Zr- $\beta$ -Zr- $\beta$ -Nb precipitate procedure is readily to happen owing to strong interactions between Nb and Nb atoms in the  $\beta$ -Zr matrix. Nevertheless, in the  $\alpha$ -Zr matrix, the interactions of foreign Nb atoms are weak due to their small binding energies, suggesting that the  $\alpha$ -Zr- $\alpha$ -Nb- $\beta$ -Nb precipitate procedure is difficult to take place. In addition, we have also provided the defect formation energies

**Table 3**  
The calculated energy values in eV in the bcc Zr matrix for the (i) perfect crystal, (ii) vacancy, (iii) substitutional Nb, (iv) two nearest neighbor substitutional Nb atoms, substitutional Nb atom–vacancy pair at, (v) the first nearest neighbor (NN), (vi) the second NN and (vii) the third NN distance. Black, white and dotted line circles represent Zr atom, Nb atom and vacancy, respectively.

Configuration	Energy per cell	Energy per atom	Formation energy	Binding energy	Previous work
 (i)	−450.97	−8.35	−	−	−8.36 [20]
 (ii)	−442.26	−	0.36	−	−
 (iii)	−452.74	−	0.07	−	−
 (iv)	−455.23	−	−0.58	0.72	−
 (v)	−446.81	−	−2.35	2.78	−
 (vi)	−445.06	−	−0.60	1.03	−
 (vii)	−444.61	−	−0.15	0.58	−

in bcc Nb. These data will be useful to further explain the precipitate and corrosion resistance performance of the Zr–Nb alloy used as cladding materials in a nuclear reactor.

### Acknowledgement

The financial supports from the National Natural Science Foundation of China (Grant Nos. 50471010 and 50871057) and the Program for New Century Excellent Talents in University, Ministry of Education of China, are gratefully acknowledged.

### References

- [1] J.P. Mardon, G. Garner, P. Beslu, D. Charquer, J. Senevat, in: Proceedings of the 1997 International Topic Meeting on LWR Fuel Performance (1997) 405.
- [2] G.P. Sabol, G.R. Kilp, M.G. Balfour, E. Robert, ASTM STP 1023 (1989) 227.
- [3] S.A. Aldridge, B.A. Cheadle, J. Nucl. Mater. 42 (1972) 32.
- [4] J.Y. Park, B.K. Choi, Y.H. Jeong, Y.H. Jung, J. Nucl. Mater. 340 (2005) 237.
- [5] Y.H. Jeong, H.G. Kim, D.J. Kim, B.K. Choi, J.H. Kim, J. Nucl. Mater. 323 (2003) 72.
- [6] V.F. Urbanic, M. Griffiths, B. Cox, R. Adamson, Y. Hatano, in: G.P. Sabol, G.D. Moan (Eds.), Proceedings of the Twelfth International Symposium on Zirconium in the Nuclear Industry, ASTM STP 1354 (2000) 641.
- [7] Y.H. Jeong, H.G. Kim, T.H. Kim, J. Nucl. Mater. 317 (2003) 1.
- [8] O.T. Woo, G.M. McDougall, R.M. Hutcheon, et al., in: G.P. Sabol, G.D. Moan (Eds.), Proceedings of the Twelfth International Symposium on Zirconium in the Nuclear Industry, ASTM STP 1354 (2000) 709.
- [9] C.D. Cann, C.B. So, R.C. Styles, C.E. Coleman, J. Nucl. Mater. 205 (1993) 267.
- [10] S. Banerjee, S.J. Vijayakar, R. Krishnan, J. Nucl. Mater. 62 (1976) 229.
- [11] O.T. Woo, R.M. Hutcheon, C.E. Coleman, in: Symposium on Microstructure of Irradiated Materials, (1995) 189.
- [12] Y.S. Kim, K.S. Im, Y.M. Cheong, S.B. Ahn, J. Nucl. Mater. 346 (2005) 120.
- [13] R.A. Perez, M. Weissmann, J. Nucl. Mater. 374 (2008) 95.
- [14] C. Domain, J. Nucl. Mater. 351 (2006) 1.
- [15] C. Domain, A. Legris, Philos. Mag. 85 (2005) 569.
- [16] R. Passianot, A.M. Monti, J. Nucl. Mater. 264 (1999) 198.
- [17] G. Kresse, J. Hafner, Phys. Rev. B 47 (1993) 558.
- [18] G. Kresse, J. Furthmuller, Phys. Rev. B 54 (1996) 11169.
- [19] H.J. Monkhorst, J.D. Pack, Phys. Rev. B 13 (1976) 5188.
- [20] Y. Wang, S. Curtarolo, C. Jiang, R. Arroyave, T. Wang, G. Ceder, L.Q. Chen, Z.K. Liu, CALPHAD 28 (2004) 79.
- [21] K. Maier, M. Peo, B. Saile, H.E. Schaefer, A. Seeger, Philos. Mag. A 40 (1979) 701.
- [22] F. Soisson, C.C. Fu, Phys. Rev. B 76 (2007) 214102.